Songklanakarin J. Sci. Technol.
42 (2), 321-328, Mar. - Apr. 2020

http://www.sjst.psu.ac.th

Original Article

Processing, properties, and biodegradation of cassava-starch cushion foam: Effects of kaolin content

Supranee Kaewpirom* and Kamolnate Sungbuakaew

Department of Chemistry, Faculty of Science,
Burapha University, Mueang, Chon Buri, 20131 Thailand

Received: 13 November 2018; Revised: 10 December 2018; Accepted: 18 December 2018

Abstract

This study aims to alter the drawbacks of starch-based foam that include poor mechanical properties and high water absorption. Biodegradable cassava-starch cushion foams were prepared successfully by compression. Kaolin was selected as a reinforcing agent as well as a water resistance additive. All of the prepared foams showed a smooth and dense outer surface with high open-cell content inside. Elongation at break of the foams decreased (from 7.1 to 2.6%), while the bending modulus increased from 66 to 112 MPa with increasing kaolin content from 0 to 15 phr. The melting temperature and the glass transition of the foam decreased from 156 to 150 °C and from 62 to 60 °C, respectively, after the addition of kaolin at 15 phr. At 100% RH, the addition of 15 phr of kaolin could reduce the equilibrium moisture content of the foam by 22% and the foam can be assimilated into the environment within a short period of time.

Keywords: cassava starch, starch-based foam, cushion foam, kaolin, biodegradation

1. Introduction

Cushioning packaging is a packaging system that protects the things inside from damage during handling and transportation. With good mechanical properties, lightweight and relatively low cost, expanded polystyrene foam (EPS) has been an attractive choice of cushion materials for consumers globally. However, owing to its non-biodegradability, EPS can create ecological problems (Mitrus & Moscicki, 2014). Therefore, replacing EPS with biodegradable foam packaging materials has become an attention-grabbing idea.

Among bio-based and biodegradable or green composites developed for use as packaging materials, starch-based composites are one of the most eye-catching alternatives to EPS. This is because starch is a renewable and sustainable raw material that biodegrades without toxic residues (Abdul Khalil *et al.*, 2014; Ashogbon & Akintayo, 2014). Therefore, it allows treatment through organic recycling and reduces landfill disposal. Among these green processing technologies, baking is recognized as a low processing cost and easy method to produce starch-based foams (Soykeabkaew, Thanomsilp, & Suwantong, 2015). Generally, the cellular structures of the cushioning materials govern their cushioning property through the stress distribution and the increased energy absorption (Xie *et al.*, 2018). However, starch-foam typically exhibited a sandwich-type structure with small, dense cells at the exterior and large cells in the interior, resulting in its poor mechanical properties. Moreover, the limitation of using starch-based foam products is their high moisture absorption due to the hydrophilic character of starch. Such high moisture absorption softens the cell structure of the foam products and weakens them.

Several techniques have been developed by various researchers to make starch foam more hydrophobic with enhanced mechanical properties. Bergel, Machado da Luz, and Santana (2018), successfully applied poly(lactic acid) coating on potato starch foam. The foam with coating presented better mechanical properties and water absorption compared to the foam without coating. Modification of the starch itself to make it more hydrophobic via the crosslinking of the hydroxyl groups by dialdehydes has been explored by Uslu and Polat (2012). With this method, food packaging trays prepared from

*Corresponding author
Email address: kaewpiro@buu.ac.th

corn starch showed the reduction in water absorption with improved flexibility. A hydrophobic/hydrophilic filler system was also composited with cassava starch foam (CSF) to amplify the water resistance of the foam. Sanhawong, Banhalee, Boonsang, and Kaewpirom (2017) proved that with the addition of an appropriate amount of both cotton fiber and concentrated natural rubber latex, the reduction of moisture absorption capacity as well as the enhanced flexural properties of cassava starch biofoam could be achieved. Moreover, Kaewtatip, Chiarathanakit, and Riyajan (2018) reported that the impact strength of baked CSF could be enhanced by the addition of egg-shell and shrimp-shell powder.

Furthermore, biocomposites based on clays or layered silicates and biodegradable polymers showed impressive improvements in the moduli, strength, and degradability compared with virgin polymers (Ojijo & Ray, 2013). Therefore, the addition of natural or modified clay is accepted as one of the effective methods to increase modulus and water resistance of starch-based foam (Lee & Hanna, 2008). Kaolin, a natural clay, is recognized as an environmentally acceptable filler that is expected to improve physical and mechanical properties of the starch foam. Kaolin is a naturally occurring material, ecologically friendly, and cost-effective. Kaewtatip, Tanrattanakul, and Phetrat (2013) incorporated kaolin into starch foam and proved that with 15 parts per hundred rubber (phr) of kaolin (CSA-15K) (dry starch basis), the izod impact strength of the CSF increased about 5 times compared with the foam without kaolin. Furthermore, they found that kaolin hindered water absorption of the CSF. Still, a limited number of publications have reported the effects of native kaolin on the physical, mechanical, and biodegradation behavior of CSF.

The key objective of this study was to produce an alternative biodegradable CSF with enhanced water resistance and mechanical strength. The foam products were prepared by the compression molding technique using water as a green solvent, a processing aid, and a blowing agent. We compared the properties of the neat CSF with CSF incorporated with fixed amounts of additives, i.e. magnesium stearate, guar gum, beeswax, and glycerol. The effects of kaolin content on the morphology, thermal, physical, and mechanical properties of the CSF were also investigated. Finally, the biodegradation behavior of a selected CSF was inspected by soil burial test.

2. Experimental

2.1 Materials

Cassava starch was purchased from Bangkok Interfood Co., Ltd. Guar gum, beeswax, kaolin, and magnesium stearate (food-grade) were purchased from Chemipan Co., Ltd. Glycerol (analytical grade) was purchased from Orec.

2.2 Preparation of cassava-starch foam

Various formulations of cassava-starch foam were prepared via compression (Table 1). Starch, distilled water, and all additives were mixed using a kitchen aid mixer at room temperature. When a homogenous batter was obtained, the batter was poured in to a 300×300×3 mm^3 mold, which was placed in a compression molding machine. The mold temperature was set at 220 °C. The process was carried out at a pressure of 1000 atm for 4.5 min.

2.3 Characterization

Foam density was calculated from the ratio of weight and volume (calculated from the apparent dimension) of a specimen. The specimens were conditioned at a relative humidity (RH) of 50% at room temperature for 14 days prior to testing. The averaged values of density of five specimens were reported for each sample.

The cross-sectional morphology of cassava-starch foam was investigated using scanning electron microscopy (SEM). A dried sample was mounted on a metal stub using a double-sided adhesive carbon tape and was coated with gold. SEM micrographs of the foam were recorded using a LEO-1450VP SEM.

The functional groups presented in the CSF were analyzed by Fourier-transform infrared (FTIR) spectroscopy (model system 2000 FTIR, Perkin Elmer) at wavenumbers 400 to 4000 cm^{-1}.

Equilibrium moisture content (EMC) of a CSF was carried out following American Association of Cereal Chemists (AACC) method 44-15A. A starch foam specimen (25.4×76.2 ×3 mm^3) was equilibrated at 0, 50, 75, and 100% RH and 30 °C for 7 days, and then weighed (W_1), followed by drying at 130 °C for 24 h in a hot air oven before another weighing (W_0) was carried out. EMC was calculated using Equation 1 and averaged values of EMC of 3 specimens were reported for each sample.

$$EMC = \frac{W_1 - W_0}{W_0} \times 100 \quad (1)$$

The thermal transitions of a dry foam sample were investigated by differential scanning calorimetry (DSC) (PYRIS Diamond DSC, Perkin Elmer). The DSC measurements were carried out from 0 to 200 °C at a heating rate of 20 °C/min with a N_2 flow rate of 40 mL/min.

Mechanical properties of the composite films were performed on a universal tensile tester (Testometric, Micro 350), with a 50 N load cell. The CSF specimens were cut into 25 mm wide and 125 mm long strips and their thicknesses were measured using a digital micrometer. Grip separation and a cross-head speed were set at 10 mm and 2 mm/min, respectively. The tests were carried out at 23 °C and 55% RH. At least 10 specimens were measured and the averaged values of Young's modulus and elongation at break (%E) were reported. Flexural properties were also inspected using the same instrument in 3-point bending mode. The support span and cross-head speed were set at 60 mm and 1 mm/min, respectively. At

Table 1. Compositions of the starting materials used to prepare the cassava starch foams[(a)].

Sample name	Cassava starch (g)	Kaolin (g)	Other additives (g)	Distilled water (mL)
Neat CSF	100	0	0	80
CSA	100	0	a	90
CSA-5K	100	5	a	90
CSA-10K	100	10	a	95
CSA-15K	100	15	a	95

[a]Other additives, i.e. guar gum (1 g), magnesium stearate (2 g), beeswax (5 g), and glycerol (4 mL) were added at fixed quantities for all foam formulae

least 10 specimens were tested, and the averaged values of the bending modulus and elongation at break were calculated.

2.4 Biodegradation test

A soil burial test was carried out on a laboratory scale. A specimen with the dimensions of 30×30×3 mm^3 was buried approximately 10 cm from the soil surface in a plastic cup containing gardening soil. The soil water content was controlled at 40–50%. The pH and temperatures of the soil were 6.6 and 21–26 °C, respectively. Digital photographs of the tested specimen were recorded intermittently.

3. Results and Discussion

3.1 Foam processing

Along with the type of starch and chemical modification, the processing condition is an important factor that affects the properties of starch-based foam (Chaudhary *et al.*, 2008). Owing to its high glass transition temperature, high viscosity, and complex gelatinization, the processing of starch is complicated and difficult to control. However, with proper formulations and suitable processing conditions, starch-based foam can be successfully produced. In this study, conventional compression molding was used to produce rigid CSF. The formulation included: 1) using a green blowing agent (water); 2) adding a mold-releasing agent (magnesium stearate) and stabilizer (guar gum); 3) blending with a hydrophobic filler (beeswax) and a plasticizer (glycerol); and 4) reinforcing with natural clay powder (kaolin). This not only fulfills the achievement of preparing biodegradable foam from native cassava starch, but also allows the use of existing machinery and potentially lowers industrial sector investment.

3.2 Foam density

Density is one of the factors that not only determines the mechanical properties of cellular cushioning materials, but also affects the shipping cost to some extent. The bulk density of CSF ranges from 0.145 to 0.165 g/cm^3 and does not significantly change with the addition of additives (Figure 1). These values are 8 to 10 times higher than commercial EPS (Xie *et al.*, 2018) and 24–31% lower than paperboard (0.21 g/cm^3) (Shey, Iman, Glenn, & Orts, 2006). However, the values are typical for CSF composites (Kaisangsri, Kerdchoechuen, & Laohakunjit, 2012; Machado, Benelli, & Tessaro, 2017). The results proved that our products were denser than EPS because of a large difference in density between polystyrene and starch. However, since starch foam is completely biodegradable, it is an attractive alternative choice for cushioning.

Unlike the density, the foam's thickness was reduced significantly (–19% reduction) as the additives were added (from 4.2 mm for neat CSF to 3.4 mm for CSA-15K). This occurred because the addition of additives created an increase in the viscosity of the starch batter. Typically, the expansion of foam products is attributed to the escape of water steam from the batter during processing (Mitrus & Moscicki, 2014). At a low viscosity, water easily escapes from the starch-batter system which creates many voids inside the gelatinized starch. The result is an increased thickness of the foam. Conversely, as the amount of an additive increases, the viscosity of the batter became relatively higher which leads to difficult release of the water molecules from the gelatinized starch. Consequently, the thickness of a starch foam product diminishes.

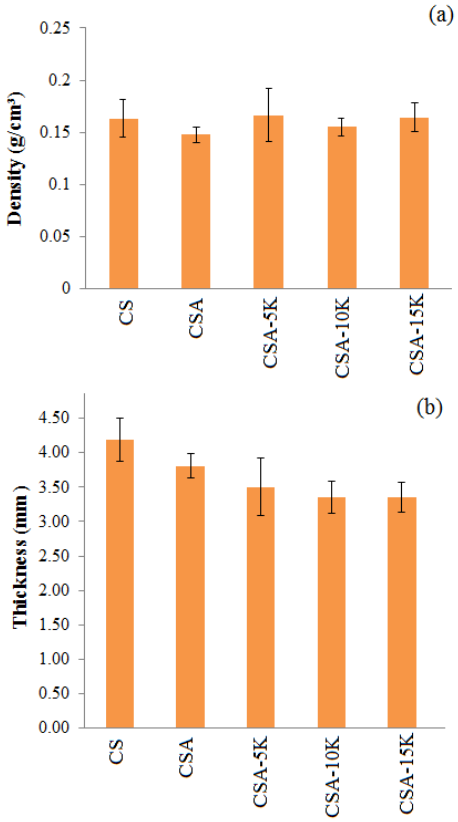

Figure 1. Bulk density of the cassava starch foams (a) and the related thickness (b).

3.3 Micro-morphology by SEM

The foam exhibited a sandwich-type structure with small, dense closed cells at the exterior and large, expanded open-cells in the interior which is typical for starch foams prepared by compression (Machado, Benelli, & Tessaro, 2017; Pornsuksomboon, Holló, Szécsényi, & Kaewtatip, 2016; Sanhawong, Banhalee, Boonsang, & Kaewpirom, 2017) (Figure 2). The neat CSF showed a smooth and dense outer surface with high open-cell content inside. This occurred because at 220 °C, a starch-water batter was locked inside a closed mold. At the outer surface, the batter was in contact with the hot mold which allowed a rapid loss of water from the gelatinized foam surface. As a result, the outer skin of the foam was dense (Song, 2016). The relatively slow evaporation of water from the interior, at which the temperature was relatively lower, resulted in a less dense interior with large open cells. With the addition of additives, a slightly rough outer surface was obtained for the CSA foams, while the high open-cell content remained. When 5 phr of kaolin was composited into the CSF (CSA-5K), the rough outer surface was clearly in evidence. Furthermore, the surface roughness increased as the content of kaolin increased. This occurred because at higher loadings, good dispersion of the kaolin particles was difficult to obtain. The kaolin particles

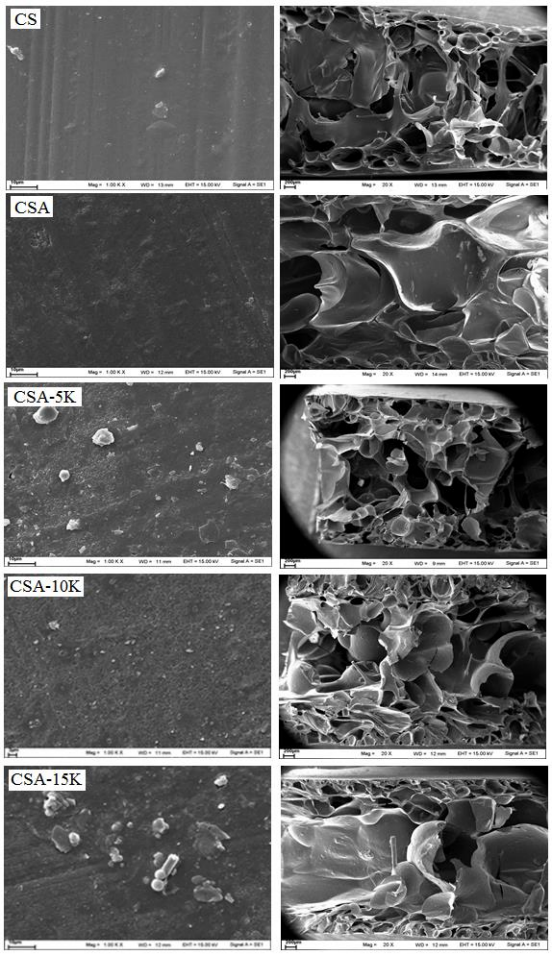

Figure 2. SEM images of surface (left) and side view (right) of the cassava starch foams.

tended to aggregrate, leading to large-sized agglomerates and high viscosity of the starch batter which affected the nucleation and growth of the bubbles in the gas-foaming process. Hence, large open cells were obviously observed at the interior, while small and elongated closed cells were found at the exterior.

3.4 Chemical structure

The functional groups present in the CSF were detected by FTIR (Figure 3). The characteristic bands of CSF are those at 3430 cm^{-1} which corresponded to O–H stretching vibration, and at 2928 cm^{-1} which was associated with the sp^3 carbon in the CH group. Absorption of the stretching vibration of the carbon bonded to a hydroxyl (C–OH) is evidenced at a wavenumber of 1150 cm^{-1} (Oliveira *et al.*, 2017). Peaks at 1638 and 1380 cm^{-1} correspond to C–O–C and H–OH stretching, respectively (Kaewtatip & Tanrattanakul, 2008). FTIR spectra of the CSA formulations were very similar to those of the neat CSF. On the other hand, FTIR spectra of the CSA-15K showed a combination of kaolin and cassava starch characteristics. A new band at 3688 cm^{-1} was attributed to kaolinite. The slight shift of the OH band to a higher wavenumber indicated the formation of hydrogen bonding the between starch and kaolin

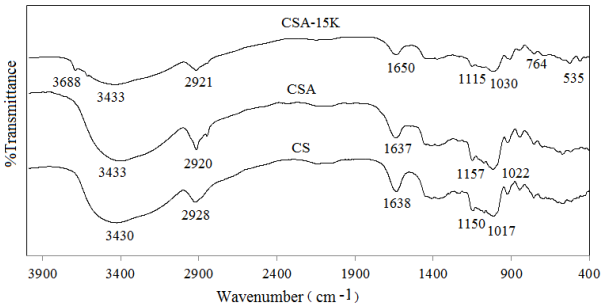

Figure 3. FTIR spectra of cassava-starch foams, namely neat CSF, CSA, and CSA-15K.

molecules. Moreover, a characteristic band of kaolin was found at 535 cm^{-1} which was attributed to Si–O–Al (Samet, Khmiri, & Chaabouni, 2013).

3.5 Thermal transition

DSC curves of the prepared CSF formulations were measured (Figure 4). Without any thermal pretreatment, the DSC thermogram of the neat CSF showed a broad endothermic peak at 156 °C. The peak refers to a prolonged water evaporation joined with the melting, due to the fusion of the different crystal regions of starch granules (Kaewtatip *et al.*, 2010). It was also reported by many authors that this typical peak was due to the crystalline melting in the native starch and only found in the first DSC heating scan (Kaewtatip & Tanrattanakul, 2008). In this study, we also found a glass transition of native starch at 66 °C. This value is in good agreement with the value reported in the literature (García *et al.*, 2012; Zeleznak & Hoseney, 1987). A shift to the lower temperatures of both glass transition (66 °C to 61 °C) and melting temperature (156 °C to 149 °C) was found in the CSA sample. This was believed to be the influence of the additives that not only separated the starch molecules from one another, but also assisted the flow of starch molecules. Hence, the peaks were wider and shifted to lower temperatures compared with the neat CSF. On the other hand, with further addition of kaolin, the glass transition and melting temperatures of CSA-15K were detected at 60 °C and 150 °C, respectively. This implied that further addition of kaolin did not significantly change the transition behavior of CSA. Kaolin cannot act as a plasticizer, but it is a reinforcing material. However, the broad melting endothermic peak of CSA-15K proved that kaolin particles can retard the crystallization process of starch molecules via hydrogen bonding between the kaolin and starch molecules.

3.6 Equilibrium moisture absorption

The equilibrium moisture absorption measurement was carried out and the results are displayed in Figure 5. As expected, the percentage of EMC of all CSF formulations increased as the RH increased. Generally, starch molecules contain plenty of water binding sites. The amorphous regions of the starch consist of both amylose and amylopectin in a disordered conformation. This allows water molecules to penetrate into the starch structure. At a low RH, the water vapor pressure is low and only a small number of water molecules can penetrate into the amorphous region of the starch which results in a

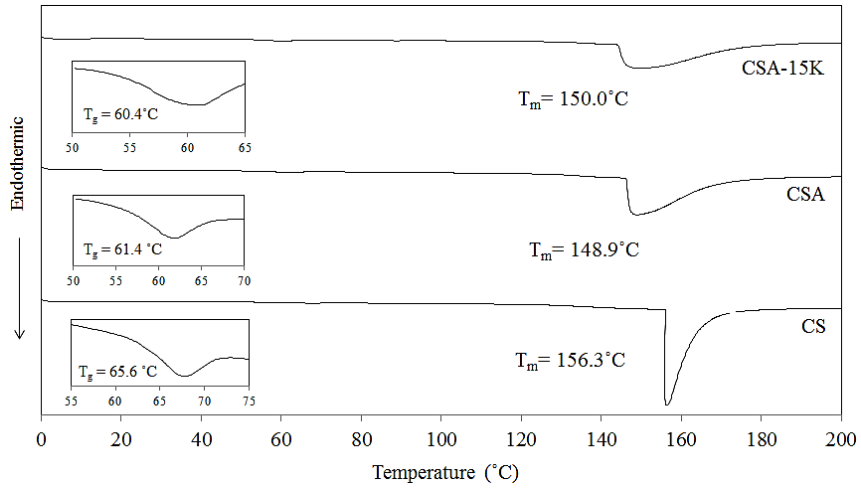

Figure 4. DSC thermograms of cassava-starch foams namely neat CSF, CSA, and CSA-15K.

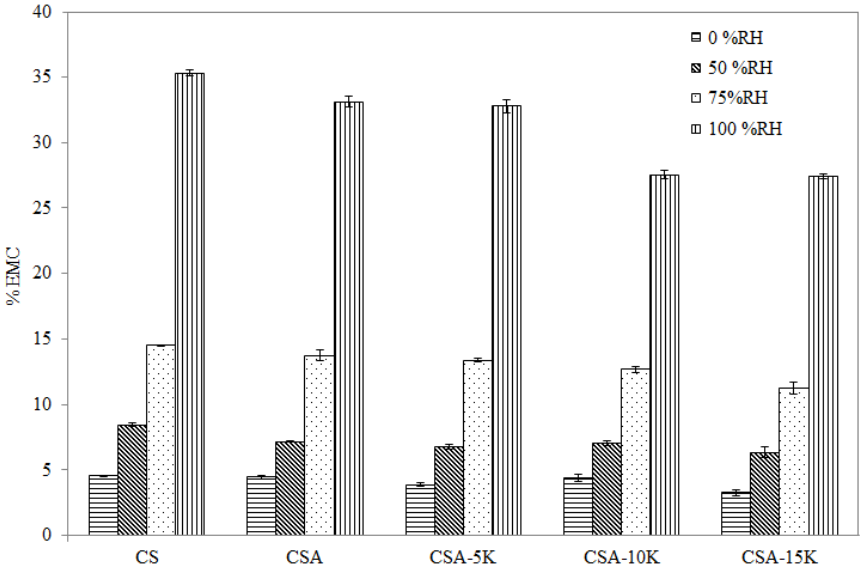

Figure 5. Equilibrium moisture content of the cassava-starch foams at 0, 50, 75, and 100% RH.

low penetration rate of water molecules. Therefore, the percentage of EMC was relatively low. Conversely, at a high RH, the water vapor pressure is high which allows plenty of water molecules to penetrate into the starch structure. Hence, the water uptake is more prominent at a high RH. The effects of adding fixed amounts of additives and kaolin content on the percentage of EMC were also investigated. At 0, 50, and 75% RH environments, the results showed no significant differences in the percentage of EMC between the neat CSF and those with additives. This occurred because at a low RH, there were only limited freely available hydroxyl groups in the starch foam. Hydrogen bonding between the starch and additive molecules plays an important force against the low vapor pressure in the adsorption mechanism (Yee, Sin, Rahman, & Samad, 2011). At a 100% RH environment, the high water vapor pressure surmounts the hydrogen bonding in the composites which causes a rise in the freely available hydroxyl groups. However, as the kaolin content increases, the number of hydrogen bonding sites significantly increases which results in a decrease in the percentage of the EMC. The addition of 15 phr of kaolin reduced the EMC of the foam by 22% compared with the neat CSF. Conclusively, kaolin plays an important role in the decreased moisture uptake of the starch foam.

3.7 Mechanical properties

Young's modulus (a) and elongation at break (b) of the cassava-starch foams are illustrated in Figure 6. As expected, the neat CSF exhibited the lowest modulus (18 MPa) with the highest elongation at break (3.6%) among all of the foam formulations. The increased modulus (+76%) and the decreased elongation at break (–47%) was found in the CSA. The addition of kaolin further increased the moduli of the CSA-5K and CSA-15K by +194% and +312%, respectively, while decreasing the elongation at break by –75% and –80%, respectively. The reason for such improvement in modulus was

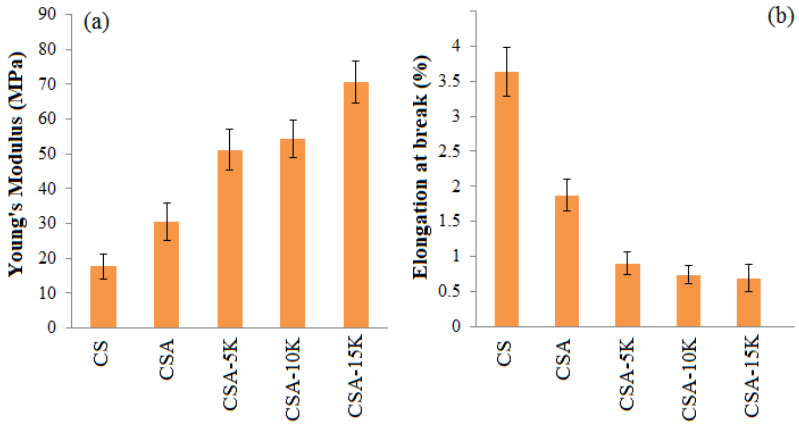

Figure 6. Tensile testing results showing Young's modulus (a) and elongation at break (b) of the cassava starch foams.

attributed to the reinforcing effect produced over the starch matrix. Hydrogen bonding between the starch and kaolin molecules made an adequate stress transfer from the starch matrix to the kaolin during tensile testing. A similar explanation can also be applied for the decrease in elongation at break. The effect of the filler on the elongation at break of the CSF formulations is possibly due to the stiffening property of the starch foam caused by intermolecular interaction between the starch chains and kaolin particles. Additionally, the decrease in molecular mobility was due to extensive formation of hydrogen bonding between the kaolin particles and starch chains that harden the matrix (Phuchaduek, Jamnongkan, Rattanasak, Boonsang, & Kaewpirom, 2015). Hence, the starch-kaolin interactions caused limited movement of the starch chains which resulted in deterioration in the flexibility of the starch foams. The effect of kaolin on the mechanical properties of the cassava starch biofoams was also confirmed by a flexural test in 3-point bending mode (Figure 7). Similar to the results obtained from tensile testing, the neat CSF displayed the lowest bending modulus (66 MPa) with the highest elongation at break (7.1%). An increased bending modulus of +62% and decreased elongation at break of –27% were found for CSA. When 5 phr of kaolin was added, the bending modulus dropped to 65 MPa, while the elongation at break dropped to 6.2%. With further addition of kaolin (10 and 15 phr), the bending modulus tended to increase, while the elongation at break tended to decrease accordingly due to the reinforcing effect.

3.8 Biodegradation

The level of biodegradation can be affected greatly by a number of parameters (Pagga, 1997). The biodegradability of a substance depends principally on its molecular structure, the environmental conditions, e.g., humidity, temperature, and diverse enzymes located in several species of micro-organisms which lead to the final mineralization of substances (Baidurah *et al.*, 2012). Since in-lab methods can be customized to the problem situation and are relatively low cost, in this study the biodegradability of a selected CSF, namely CSA-15K, was investigated qualitatively by a soil burial test. Unfortunately, the weight change of CSA-15K was not measured because of the association of the biomass in the soil which led to an overestimation of the sample weight.

A digital photograph of the tested specimen showed the association of the biomass in the soil with the foam surface after one day in the soil burial test (Figure 8). This was attributed to the quick soil water sorption caused by plenty of hydroxyl groups in the foam structure. The hydroxyl groups of starch molecules interacted with the soil and water which led to the destruction of the starch-kaolinite hydrogen bonding as well as hydrogen bonding and molecular interaction between the starch molecules themselves. As a consequence, the CSA-15K swelled and was prone to degradation. Degradation supposedly started after swelling and the rupture was noticed clearly after 3 days of the test. This confirmed that at the early stage of degradation, the CSF could degrade in soil via hydrolysis. Later, we believed that biodegradation of the foam occurred with enzymatic action that involved living microorganisms in the gardening soil. Molecular degradation was promoted further by enzymes which led to complete or partial removal of the foam from the environment. At week 3, the foam and biomass were not distinguishable in the soil. Therefore, the waste of CSF produced in this study can be simply disposed in gardens, in which carbon- and nitrogen-rich components are supplemented to provide boosted conditions for microbial growth.

4. Conclusions

An alternative biodegradable CSF was successfully prepared by compression using water as the green blowing agent. The properties of the neat CSF were effectively improved by the incorporation of magnesium stearate, guar gum, beeswax, glycerol, and kaolin. The rigidity and dimensional stability in contact with water can be tremendously improved by the incorporation of kaolin. Although the modulus of CSF was low, the other properties, such as elongation and density of the foam products were comparable to those of the starch-based foams reported previously. Furthermore, the biodegradation of the foam proceeded via hydrolysis at the early stage followed by enzymatic degradation. Therefore, this material can be assimilated into the environment over a comparatively short period of time.

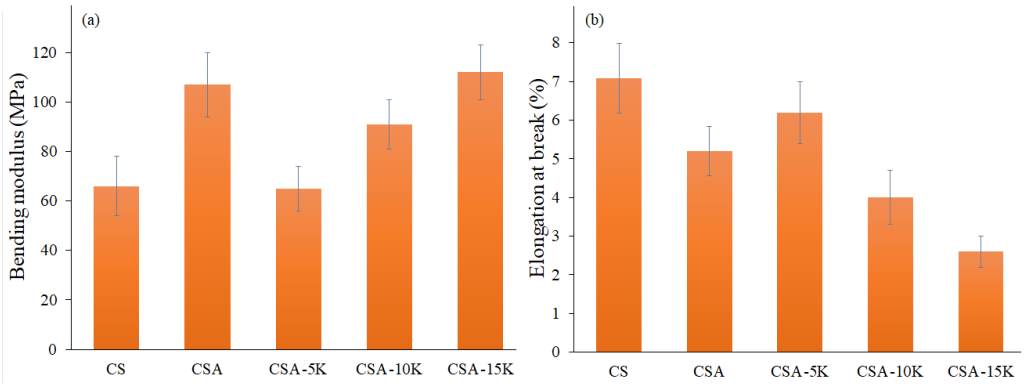

Figure 7. Flexural testing results showing bending modulus (a) and elongation at break (b) of the cassava starch foams.

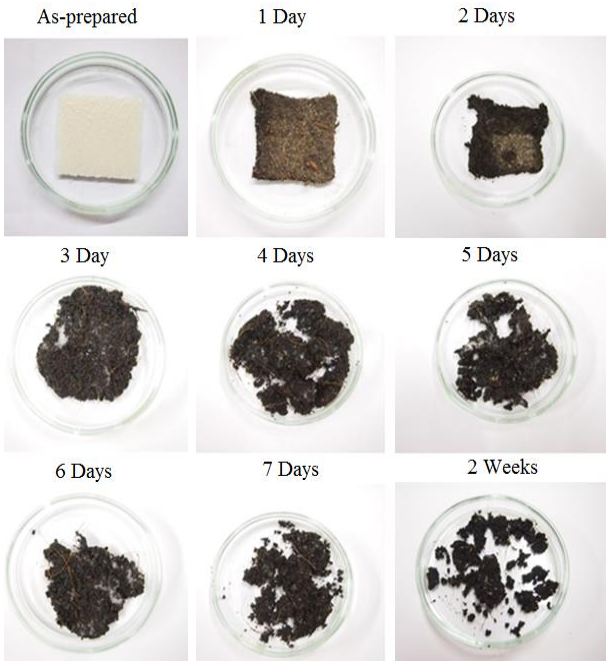

Figure 8. Digital photographs showing the degradation behavior of CSA-15K as a function of time.

Acknowledgements

This work was financially supported by the Research Grant of Burapha University through National Research Council of Thailand (Grant no. 190/2561).

References

Abdul Khalil, H. P., Davoudpour, Y., Mustapha, A., Sudesh, K., Dungani, R., & Jawaid M. (2014). Production and modification of nanofibrillated cellulose using various mechanical processes: a review. *Carbohydrate Polymers*, *99*, 649–665.

Ashogbon, A. O., & Akintayo, E. T. (2014). Recent trend in the physical and chemical modification of starches from different botanical sources: A review. *Starch–StÃrke*, *66*(1–2), 41–57.

Baidurah, S., Takada, S., Shimizu, K., Yasue, K., Arimoto, S., Ishida, Y., . . . Ohtani, H. (2012). Evaluation of biodegradability of poly(butylene succinate-*co*-butylene adipate) on the basis of copolymer composition determined by thermally assisted hydrolysis and methylation-gas chromatography. *International Journal of Polymer Analysis and Characterization*, *17*(1), 29–37.

Bergel, B. F., Machado da Luz, L., & Santana, R. M. C. (2018). Effect of poly(lactic acid) coating on mechanical and physical properties of thermoplastic starch foams from potato starch. *Progress in Organic Coatings*, *118*, 91–96.

Chaudhary, A. L., Miller, M., Torley, P. J., Sopade, P. A., & Halley, P. J. (2008). Amylose content and chemical modification effects on the extrusion of thermoplastic starch from maize. *Carbohydrate Polymers*, *74*(4), 907–913.

García, L., Cova, A., Sandoval, A. J., Müller, A. J., & Carrasquel, L. M. (2012). Glass transition temperatures of cassava starch–whey protein concentrate systems at low and intermediate water content. *Carbohydrate Polymers*, *87*(2), 1375–1382.

Kaewtatip, K., Chiarathanakit, C., & Riyajan, S. (2018). The effects of egg shell and shrimp shell on the properties of baked starch foam. *Powder Technology*, *335*, 354–359.

Kaewtatip, K., & Tanrattanakul, V. (2008). Preparation of cassava starch grafted with polystyrene by suspension polymerization. *Carbohydrate Polymers*, *73*(4), 647–655.

Kaewtatip, K., Tanrattanakul, V., & Phetrat, W. (2013). Preparation and characterization of kaolin/starch foam. *Applied Clay Science*, *80–81*, 413–416.

Kaewtatip, K., Tanrattanakul, R., Szécsényi, K. M., Pavličević, J., & Budinski-Simendic, J. (2010). Thermal properties and morphology of cassava starch grafted with different content of polystyrene. *Journal of thermal Analysis and Calorimetry*, *102*(3), 1035–1041.

Kaisangsri, N., Kerdchoechuen, O., & Laohakunjit, N. (2012). Biodegradable foam tray from cassava starch blended with natural fiber and chitosan. *Industrial Crops and Products*, *37*(1), 542–546.

Lee, S. Y., & Hanna, M. A. (2008). Preparation and characterization of tapioca starch/poly(lactic acid)-Cloisite NA^+ nanocomposite foams. *Journal of Applied Polymer Science, 110*, 2337–2344.

Machado, C. M., Benelli, P., & Tessaro, I. C. (2017). Sesame cake incorporation on cassava starch foams for packaging use. *Industrial Crops and Products, 102*, 115–121.

Mbey, J. A., & Thomas, F. (2015). Components interactions controlling starch–kaolinite composite films properties. *Carbohydrate Polymers*, 117, 739–745.

Mitrus, M., & Moscicki, L. (2014). Extrusion-cooking of starch protective loose-fill foams. *Chemical Engineering Research and Design, 92*(4), 778–783.

Ojijo, V., & Ray, S. S. (2013). Processing strategies in bionanocomposites. *Progress in Polymer Science, 38*(10–11), 1543–1589.

Oliveira, T. A., Oliveira, R. R., Barbosa, R., Azevedo, J. B., & Alves, T. S. (2017). Effect of reprocessing cycles on the degradation of PP/PBAT-thermoplastic starch blends. *Carbohydrate Polymers, 168*, 52–60.

Pagga, U. (1997). Testing biodegradability with standardized methods. *Chemosphere, 35*(12), 2953–2972.

Phuchaduek, W., Jamnongkan, T., Rattanasak, U., Boonsang, S., & Kaewpirom, S. (2015). Improvement in physical and electrical properties of poly(vinyl alcohol) hydrogel conductive polymer composites. *Journal of Applied Polymer Science, 132*(28).

Pornsuksomboon, K., Holló, B. B., Szécsényi, K. M., & Kaewtatip, K. (2016). Properties of baked foams from citric acid modified cassava starch and native cassava starch blends. *Carbohydrate Polymers, 136*, 107–112.

Salgado, P. R., Schmidt, V. C., Molina, S. E., & Mauri, A. N. J. (2008). Biodegradable foams based on cassava starch, sunflower proteins and cellulose fibers obtained by baking process. *Journal of Food Engineering, 85*, 435–443.

Samet, B., Khmiri, A., & Chaabouni, M. (2013). Chemical behaviour of ground waste glass when used as partial cement replacement in mortars. *Construction and Building Materials, 44*, 74–80.

Sanhawong, W., Banhalee, P., Boonsang, S., & Kaewpirom, S. (2017). Effect of concentrated natural rubber latex on the properties and degradation behavior of cotton-fiber-reinforced cassava starch biofoam. *Industrial Crops and Products, 108*, 756–766.

Shey, J., Imam, S. H., Glenn, G. M., & Orts, W. J. (2006). Properties of baked starch foam with natural rubber latex. *Industrial Crops and Products, 24*(1), 34–40.

Song, J. (2016). Starch foam. In S. Iannace & C. B. Park (Eds.), *Biofoams: Science and Applications of Bio-Based Cellular and Porous Materials* (pp. 207–226). Boca Raton, FL: CRC Press.

Soykeabkaew, N., Thanomsilp, C., & Suwantong, O. (2015). A review: Starch-based composite foams. *Composites Part A: Applied Science and Manufacturing, 78*, 246–263.

Uslu, M. K., & Polat, S. (2012). Effects of glyoxal cross-linking on baked starch foam. *Carbohydrate Polymers, 87*(3), 1994–1999.

Xie, Q., Li, F., Li, J., Wang, L., Li, Y., Zhang, C., . . . Chen, S. (2018). A new biodegradable sisal fiber-starch packing composites with nest structure. *Carbohydrate Polymers, 189*, 56–64.

Yee, T. W., Sin, L. T., Rahman, W. A. W. A., & Samad, A. A. (2011). Properties and interactions of poly(vinyl alcohol)sago pith waste biocomposites. *Journal of Composite Materials, 45*(21), 2199–2203.

Zeleznak, K. J., & Hoseney, R. C. (1987). The glass transition in starch. *Cereal Chemistry, 64*(2), 121–124.